

# Unprecedented Superconductivity in the $\beta$ -Pyrochlore Osmate $\text{KOs}_2\text{O}_6$

Z. Hiroi, S. Yonezawa, and Y. Muraoka

Institute for Solid State Physics, University of Tokyo, Kashiwa, Chiba 277-8581, Japan

Superconductivity in the potassium osmium oxide  $\text{KOs}_2\text{O}_6$  crystallizing in the  $\beta$ -pyrochlore structure is studied by means of electrical resistivity, magnetic susceptibility and specific heat. The superconducting transition temperature is 9.6 K, and the upper critical magnetic field is about 38 T, which seems to exceed Pauli's limit expected for conventional superconductivity. The observed peculiar temperature dependences of resistivity and magnetic susceptibility indicate that the superconductivity occurs in a strongly correlated and highly frustrated electron system with large antiferromagnetic spin fluctuations on the triangle-based pyrochlore lattice.

74.70.-b, 74.25.Bt, 71.27.+a, 75.40.-s

The huge number of electrons in a condensed matter system often form pairs in their ground state. The phenomenon of superconductivity presents one example, in which such Cooper pairs of electrons carry a resistance-free current at temperature below a critical temperature  $T_c$ . Stable Cooper pairs exist on square lattices such as the  $\text{CuO}_2$  plane found in copper oxide superconductors, as reflected in their extremely high values of  $T_c$ . In contrast, superconductivity is not thought to be preferred on triangle-based lattices, and would be exotic if it exists, because of the essential difference of

such non-bipartite lattices from the square lattice. Previously, superconductivity with  $T_c = 1$  K was found on the triangle-based pyrochlore lattice, which is formed from corner-sharing tetrahedra, in  $\text{Cd}_2\text{Re}_2\text{O}_7$  [1-3]. It is the first superconductor in the family of pyrochlore oxides which constitute a large group of transition metal (TM) oxides [4]. Unexpectedly, the mechanism of the superconductivity appears to be conventional, and may be understood in the framework of the weak-coupling Bardeen-Cooper-Schrieffer (BCS) theory [5]. Recently, the triangular lattice of  $\text{CoO}_2$  in  $\text{Na}_x\text{CoO}_2\text{-yH}_2\text{O}$  was rendered superconducting at  $T_c = 5$  K, although the mechanism for Cooper pairing remains an open question [6]. Very recently, we found another pyrochlore-based superconductor,  $\text{KO}_{\text{s}2}\text{O}_6$ , with  $T_c = 10$  K [7], a value ten times larger than in  $\text{Cd}_2\text{Re}_2\text{O}_7$ . Moreover, a related compound  $\text{Rb}_{\text{s}2}\text{O}_6$  was found to show superconductivity with  $T_c = 6.3$  K [8]. Here we report the superconducting properties of  $\text{KO}_{\text{s}2}\text{O}_6$  probed by electrical resistivity, magnetic susceptibility and specific heat measurements. Our experimental results suggest unconventional superconductivity occurring on a three-dimensional pyrochlore lattice..

Most pyrochlore oxides containing  $5d$  TM elements such as Re, Os and Ir are bad metals. The superconductor  $\text{Cd}_2\text{Re}_2\text{O}_7$ , which contains  $\text{Re}^{5+}$  ions with two  $5d$  electrons, is a good metal at low temperature below a structural phase transition at 200 K [9]. In contrast, a related pyrochlore oxide  $\text{Cd}_2\text{Os}_2\text{O}_7$  containing  $\text{Os}^{5+}$  ions with three  $5d$  electrons undergoes a metal-insulator (MI) transition at a critical temperature  $T_{\text{MI}} = 225$  K [10]. Long-range antiferromagnetic order is thought to set in simultaneously [11], although the details of the ordered structure have not yet been elucidated. The obvious difference between the two compounds lies in the number of  $d$  electrons on the B-site cations. This striking contrast illustrates the rich physics involved in the  $5d$  TM

pyrochlore oxides on the basis of electron correlations near the MI transition and frustration on the pyrochlore lattice. In this scenario, the properties of the present compound  $\text{KO}_{\text{Os}_2\text{O}_6}$  is extremely interesting, because it contains  $\text{Os}^{5.5+}$  ions with two and half d electrons, just between  $\text{Cd}_2\text{Re}_2\text{O}_7$  and  $\text{Cd}_2\text{Os}_2\text{O}_7$ .

A polycrystalline sample was prepared from  $\text{KO}_2$  and  $\text{OsO}_2$  (Alfa Aesar) by heating at 873 K for 24 h under controlled oxygen partial pressures. The product was nearly single-phase, but with a small trace of  $\text{OsO}_2$ . Our preliminary structural analysis indicates that it crystallizes in a cubic structure with space group  $Fd\text{-}3m$ , as in the ideal pyrochlore oxides [7]. Figure 1 depicts a proposed structural model for  $\text{KO}_{\text{Os}_2\text{O}_6}$ , where K atoms are located at the O' site of the ideal pyrochlore oxide  $\text{A}_2\text{B}_2\text{O}_6\text{O}'$ , and thus at the center of cages formed from  $\text{OsO}_6$  octahedra. The pyrochlore lattice structure, which is composed of corner-sharing tetrahedra, or all triangles, appears from the structure when one considers only the Os atoms, as shown in Fig. 1. At present we cannot exclude the possibility that a small structural deformation occurs in this compound, as observed in  $\text{Cd}_2\text{Re}_2\text{O}_7$  [12,13] or other  $\text{AB}_2\text{O}_6$  compounds [14]. A detailed structural investigation will be reported later.

Figure 2a shows the characteristic temperature dependence of the resistivity for  $\text{KO}_{\text{Os}_2\text{O}_6}$ . When the sample is cooled below 10 K, the resistivity drops sharply, indicating a phase transition to a superconducting state. The onset temperature is 9.8 K, and zero resistivity is attained below 8.5 K. The critical temperature  $T_c$ , defined at the midpoint of the transition, is 9.5 K. The resistivity above the transition shows a peculiar temperature dependence which is far from that expected in an ordinary metal, suggesting that anomalous scattering processes are relevant. For further discussion, however, it would be necessary to obtain alternative resistivity data from a single

crystalline sample instead of from a polycrystalline pellet. In addition to the transition to zero resistance, a large diamagnetic signal associated with the Meissner effect was observed below 9.6 K, as shown in Fig. 2b. The superconducting volume fraction estimated at 2 K from the zero-field cooling experiment is about 70 %, which is large enough to constitute bulk superconductivity.

The superconducting transition was also confirmed by heat capacity measurements. The specific heat divided by temperature for  $\text{KO}_{\text{Os}_2}\text{O}_6$  is shown in Fig. 2c, where a large jump is observed at  $T_c = 9.58$  K. The magnitude of the jump,  $\Delta C/T_c$ , is  $27.2 \text{ mJ/K}^2 \text{ mol Os}$ . We are unable to deduce the electronic component of the specific heat from this data, because there is at present no appropriate means of estimating the lattice contribution. In a conventional weak-coupling superconductor,  $\Delta C/\gamma T_c = 1.43$ , where  $\gamma$  is the Sommerfeld coefficient. Assuming this relation would yield  $\gamma = 19.0 \text{ mJ/K}^2 \text{ mol Os}$ , which is slightly larger than  $\gamma = 15.1 \text{ mJ/K}^2 \text{ mol Re}$  in  $\text{Cd}_2\text{Re}_2\text{O}_7$  [1].

Superconductivity in  $\text{KO}_{\text{Os}_2}\text{O}_6$  is remarkably robust under high magnetic fields. Figure 3 shows the specific heat of  $\text{KO}_{\text{Os}_2}\text{O}_6$  measured under various magnetic fields up to 14 T, where the jump shifts systematically to lower temperatures with increasing fields. However, even at 14 T,  $T_c$  is 7.1 K, reduced by only 2.5 K from that at zero field. The upper critical field  $H_{c2}(T)$  obtained as a function of temperature is plotted in the field-temperature diagram shown in the inset to Fig. 3, and is found to increase linearly with a large gradient as the temperature decreases. From the gradient one may estimate  $H_{c2}(0)$  at  $T = 0$ , using the Werthamer-Helfand-Hohenberg (WHH) formula proposed for a weak-coupling superconductor in the clean limit;  $H_{c2}(0) = 0.693(-d H_{c2}/dT)_{T=T_c} T_c$  [15]. This yields  $\mu_0 H_{c2}(0) = 38.3$  T, a surprisingly large value of more than twice

Pauli's limiting field  $\mu_0 H_P = 1.85 T_c = 17.8$  T. This result strongly suggests that superconductivity in  $\text{KO}_{\text{Os}_2}\text{O}_6$  is unconventional. The observed large value of  $H_{c2}$  for  $\text{KO}_{\text{Os}_2}\text{O}_6$  implies a small Ginzburg-Landau coherence length at  $T = 0$ , which is calculated to be  $\xi_{\text{GL}}(0) = 3.0$  nm, using the GL formula,  $\mu_0 H_{c2}(0) = \phi_0/(2\pi\xi_{\text{GL}}(0)^2)$ , where  $\phi_0$  is the flux quantum. These values are to be compared with the case of  $\text{Cd}_2\text{Re}_2\text{O}_7$  with  $T_c = 1$  K, where  $\mu_0 H_{c2}(0) = 0.29$  T is much smaller than  $\mu_0 H_P = 2.0$  T, and  $\xi_{\text{GL}}(0) = 34$  nm [5].

On the normal state properties of  $\text{KO}_{\text{Os}_2}\text{O}_6$ , it is to be noted that the magnetic susceptibility at high temperatures exhibits a significant temperature dependence, as shown in Fig. 4. The behavior is substantially different from temperature-independent Pauli paramagnetism for ordinary metals. The susceptibility increases gradually with decreasing temperature, and exhibits a broad maximum around  $T = 50$  K, as often seen in low-dimensional spin systems. The small upturn below 20 K may be due to the presence of impurity spins. The susceptibility at high temperatures, above the maximum, obeys the Curie-Weiss law, as is apparent from the linear temperature dependence of the inverse susceptibility shown in the figure. This fact indicates that  $\text{KO}_{\text{Os}_2}\text{O}_6$  is actually a strongly correlated metal with large electron correlations. Fitting the susceptibility to the form  $\chi = C/(T + \Theta)$  yields  $C = 0.152$  and  $\Theta = -350$  K, where  $C$  and  $\Theta$  are respectively the Curie constant and the Weiss temperature. The remarkably large Weiss temperature with negative sign implies that antiferromagnetic spin correlations are dominant. The magnitude of an effective paramagnetic moment deduced from the Curie constant is  $p_{\text{eff}} = 1.1\mu_{\text{B}}$  per Os, which is smaller than the spin-only value for 2.5  $d$  electrons ( $3.35\mu_{\text{B}}$ ).  $\text{Cd}_2\text{Os}_2\text{O}_7$  also shows a Curie-Weiss-type magnetic susceptibility at high temperature (above  $T_{\text{MI}}$ ), with  $p_{\text{eff}} = 1.3\mu_{\text{B}}$  and  $\Theta = -320$

K. In addition, it shows a distinct anomaly at  $T_{MI}$ , indicative of a phase transition to antiferromagnetic order. In contrast,  $Cd_2Re_2O_7$  has a temperature-independent susceptibility over a wide temperature range, except for a gradual reduction observed below  $T_{s1} = 200$  K which is due to a decrease in the density of states (DOS) associated with the structural phase transition [9,16-18].

The origin of the broad maximum observed in the susceptibility of  $KOs_2O_6$  remains mysterious. No corresponding anomalies in the resistivity are measured on the polycrystalline sample shown in Fig.1a. Moreover, we did not observe any anomalies in specific heat measurements, which indicates that the broad peak should not be ascribed to a phase transition. Therefore, it seems that some short-range antiferromagnetic correlation has developed between the moments at low temperature (below the maximum), or that some form of pseudo-gap has opened at the Fermi level. Elucidation of this mystery may hold the key to understanding the electronic properties and also the mechanism of superconductivity in  $KOs_2O_6$ .

It is interesting to compare  $KOs_2O_6$  with two related pyrochlore oxides,  $Cd_2Re_2O_7$  and  $Cd_2Os_2O_7$ , in terms of band filling. The previous band structure calculations on the two compounds revealed that they show semi-metallic bands with low carrier density near the Fermi energy [19,20]. There is a manifold of predominant  $t_{2g}$ -orbital character consisting of twelve bands near the Fermi energy. The total band width is approximately 3 eV, which may exceed the effective Hubbard  $U$  term, thought to be on the order of 2 eV [19]. Thus these compounds should not be classified as strongly correlated metals in an ordinary sense, and certainly  $Cd_2Re_2O_7$  exhibits simple Pauli paramagnetism. However, there are also several sharp peaks in the DOS which arise from the flatness and high degeneracy of some of the constituent bands, reflecting

the unique crystal structure of the pyrochlore oxides. The electronic properties may therefore change dramatically as a function of the electron filling. In the case of  $\text{Cd}_2\text{Re}_2\text{O}_7$ , with two  $d$  electrons per Re, the Fermi level is located near a local minimum of the DOS, while for  $\text{Cd}_2\text{Os}_2\text{O}_7$ , with three  $d$  electrons per Os, it lies in the middle of the  $t_{2g}$  manifold, where a sharp peak exists [19]. It is probable that a magnetic instability associated with this ‘half-filled’ central peak causes the metal-insulator transition observed at 225 K. In this sense, electron correlation effects in these compounds are not associated with an on-site Coulomb repulsion in a single-band model, but depends on electron filling, reflecting the muliband character of the band structure in the pyrochlore oxides [19]. It was also noted for  $\text{Cd}_2\text{Os}_2\text{O}_7$  that the semimetallic band structures consisting of very heavy hole and elecron bands may give rise to an exitonic instability of the Fermi surface [19], although in this case one would expect a ferromagnetic spin correlation in this case instead of an antiferromagnetic one.

$\text{KO}_{\text{Os}_2}\text{O}_6$  is expected to have a similar band structure, because the B-O framework is almost identical among the three compounds. Thus the electronic properties of  $\text{KO}_{\text{Os}_2}\text{O}_6$ , with two and half  $d$  electrons per Os, may be in between these two paradigms. In fact  $\text{KO}_{\text{Os}_2}\text{O}_6$  shows superconductivity as does  $\text{Cd}_2\text{Re}_2\text{O}_7$ , while its magnetism is ‘active’ as in  $\text{Cd}_2\text{Os}_2\text{O}_7$ . Nevertheless, long-range antiferromagnetic order does not occur in  $\text{KO}_{\text{Os}_2}\text{O}_6$ , possibly due to the lower DOS at the Fermi level as well as the frustration on the pyrochlore lattice of spin triangles. Because the large enhancement of  $T_c$  from  $\text{Cd}_2\text{Re}_2\text{O}_7$  to  $\text{KO}_{\text{Os}_2}\text{O}_6$  seems to be achieved by approaching the magnetic instability which is known to be present in  $\text{Cd}_2\text{Os}_2\text{O}_7$ , we expect that antiferomagnetic fluctuations on the frustrated pyrochlore lattice play an important role in the mechanism of superconductivity in  $\text{KO}_{\text{Os}_2}\text{O}_6$ .

In conclusion, we have reported the superconducting properties of the second pyrochlore oxide superconductor  $\text{KO}_{\text{Os}_2}\text{O}_6$  and suggest that unprecedented superconductivity is realized on the basis of electron correlations near the MI transition and frustration on the pyrochlore lattice. The discovery of superconductivity in  $\text{KO}_{\text{Os}_2}\text{O}_6$ , as well as in  $\text{Na}_x\text{CoO}_2\text{-yH}_2\text{O}$ , opens the door to another fascinating world of superconductivity realized on the triangle-based lattices, which must be substantially different from that on square-based lattices such as the  $\text{CuO}_2$  planes in copper oxide superconductors.

We are grateful to M. Takigawa, M. Ogata, and H. Harima for enlightening discussions. We also want to express our special thanks for B. Normand for reading our manuscript and giving us helpful comments. This research was supported by a Grant-in-Aid for Scientific Research on Priority Areas (A) provided by the Ministry of Education, Culture, Sports, Science and Technology, Japan.

## References

- [1] M. Hanawa, Y. Muraoka, T. Tayama, T. Sakakibara, J. Yamaura, and Z. Hiroi, Phys. Rev. Lett. **87**, 187001 (2001).
- [2] H. Sakai, K. Yoshimura, H. Ohno, H. Kato, S. Kambe, R.E. Walstedt, T.D. Matsuda, Y. Haga, and Y. Onuki, J. Phys.:Condens. Matter **13**, L785 (2001).
- [3] R. Jin, J. He, S. McCall, C.S. Alexander, F. Drymiotis, and D. Mandrus, Phys. Rev. B **64**, 180503 (2001).
- [4] M.A. Subramanian, G. Aravamudan, and G.V.S. Rao, Prog. Solid State Chem. **15**, 55 (1983).
- [5] Z. Hiroi, and M. Hanawa, J. Phys. Chem. Solids **63**, 1021 (2002).

- [6] K. Takada, H. Sakurai, E. Takayama-Muromachi, F. Izumi, R.A. Dilanian, and T. Sasaki, *Nature* **422**, 53 (2203).
- [7] S. Yonezawa, Y. Muraoka, Y. Matsushita, and Z. Hiroi, *J. Phys.:Condens. Matter* **16**, L9 (2004).
- [8] S. Yonezawa, Y. Muraoka, Y. Matsushita, and Z. Hiroi, *J. Phys. Soc. Jpn*, in press.
- [9] Z. Hiroi, M. Hanawa, Y. Muraoka, and H. Harima, *J. Phys. Soc. Jpn* **72**, 21 (2003).
- [10] A.W. Sleight, J.L. Gilson, J.F. Weiher, and W. Bindloss, *Solid State Commun.* **14**, 357 (1974).
- [11] D. Mandrus, J.R. Thompson, R. Gaal, L. Forro, J.C. Bryan, B.C. Chakoumakos, L.M. Woods, B.C. Sales, R.S. Fishman, and V. Keppens, *Phys. Rev. B* **63**, 195104 (2001).
- [12] J. Yamaura, and Z. Hiroi, *J. Phys. Soc. Jpn* **71**, 2598 (2002).
- [13] J.P. Castellan, B.D. Gaulin, J. van Duijn, M.J. Lewis, M.D. Lumsden, R. Jin, J. He, S.E. Nagler, and D. Mandrus, *Phys. Rev. B* **66**, 134528 (2002).
- [14] A.W. Sleight, F.C. Zumsteg, J.R. Barkley, and J.E. Gulley, *Mat. Res. Bull.* **13**, 1247 (1978).
- [15] N.R. Werthamer, E. Helfand, and P.C. Hohenberg, *Phys. Rev.* **147**, 295 (1966).
- [16] Z. Hiroi, J. Yamaura, Y. Muraoka, and M. Hanawa, *J. Phys. Soc. Jpn* **71**, 1634 (2002).
- [17] O. Vyaselev, K. Arai, K. Kobayashi, J. Yamazaki, K. Kodama, M. Takigawa, M. Hanawa, and Z. Hiroi, *Phys. Rev. Lett.* **89**, 017001 (2002).

- [18] R. Jin, J. He, J.R. Thompson, M.F. Chisholm, B.C. Sales, and D. Mandrus, *J. Phys.:Condens. Matter* **14**, L117 (2002).
- [19] D.J. Singh, P. Blaha, K. Schwarz, and J.O. Sofo, *Phys. Rev. B* **65**, 155109 (2002).
- [20] H. Harima, *J. Phys. Chem. Solids* **63**, 1035 (2002).

Figure caption

**FIG. 1.** Structural views of the pyrochlore lattice (top) and  $\text{KO}_{\text{S}_2}\text{O}_6$  (bottom). A red octahedron with six light blue balls on the vertices represents an  $\text{OsO}_6$  unit, and a dark blue ball represents a potassium atom coordinated by six oxygen atoms from neighbouring  $\text{OsO}_6$  octahedra. The crystallographic sites are  $8b$ ,  $16c$  and  $48f$  in the space group  $Fd\text{-}3m$  for K, Os and O atoms, respectively. The pyrochlore lattice emerges from the structure by considering only osmium atoms, and contains  $\text{Os}_4$  tetrahedra with each one connected to four equivalent tetrahedra by their vertices.

**FIG. 2.** Temperature dependences of resistivity ( $\rho$ ) (a), magnetization ( $M$ ) (b) and specific heat ( $C$ ) (c), showing a superconducting transition at  $T_c = 9.6$  K. Resistivity was measured by the standard four-probe method in a commercial equipment (PPMS, Quantum Design). Susceptibility measurements were carried out by a superconducting quantum interference device magnetometer (MPMS-XL, Quantum Design) in a magnetic field of 10 Oe on heating after zero-field cooling (ZFC) and then on cooling in a field (FC). Specific heat was measured by the heat relaxation method in commercial equipment (PPMS, Quantum Design). All the measurements were performed on polycrystalline samples.

**FIG. 3.** Magnetic field dependence of specific heat divided by temperature between 0 and 14 T. The inset shows a field-temperature phase diagram where the upper critical field  $H_{c2}$  determined from the specific heat measurements is plotted. ‘S’ and ‘N’ refer to superconducting and normal regions, respectively. Solid lines are guides to the eye.

**FIG. 4.** Temperature dependence of magnetic susceptibility ( $\chi$ ) measured on heating in a magnetic field of 10 kOe. The inverse susceptibility is also plotted.

**The solid line between 50 K and 300 K on the  $1/\chi$  data points is a fit to the Curie-Weiss law.**

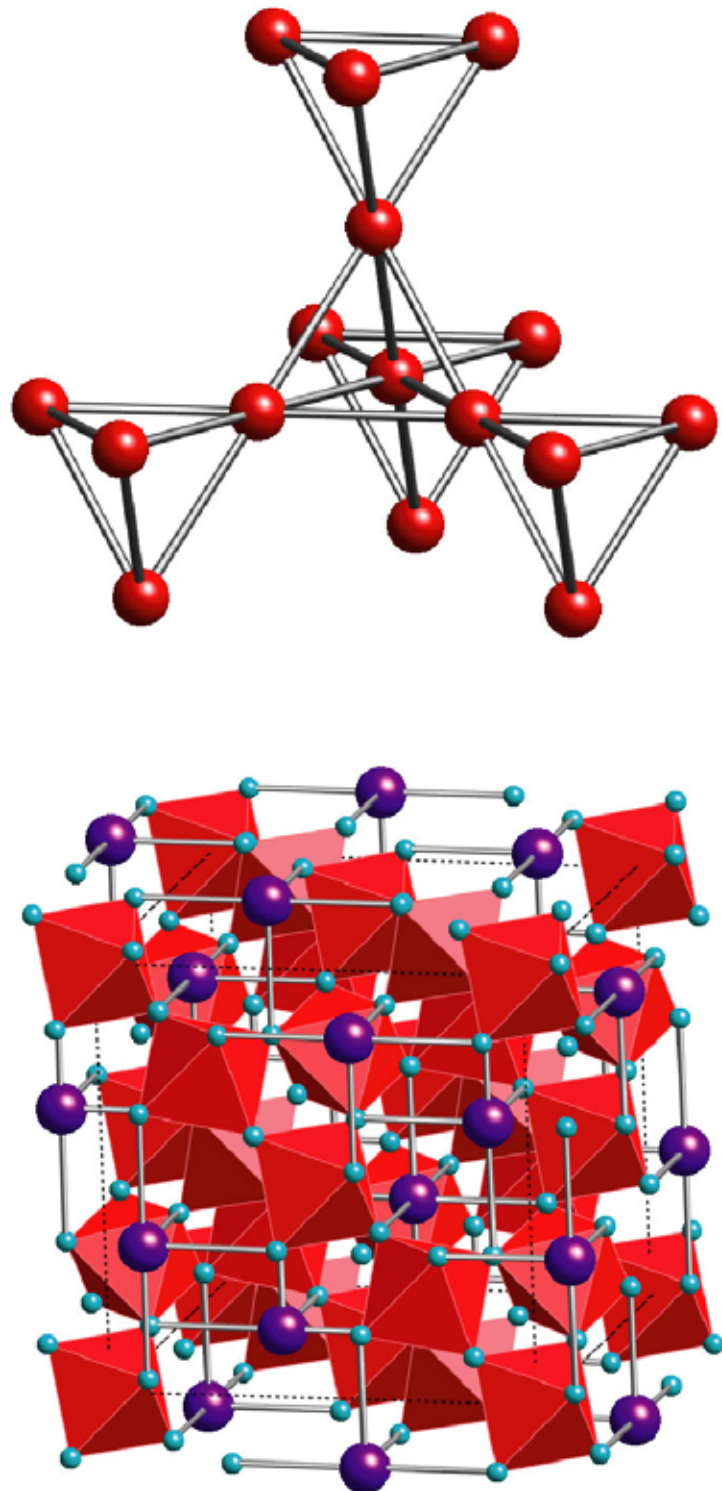


FIG. 1.

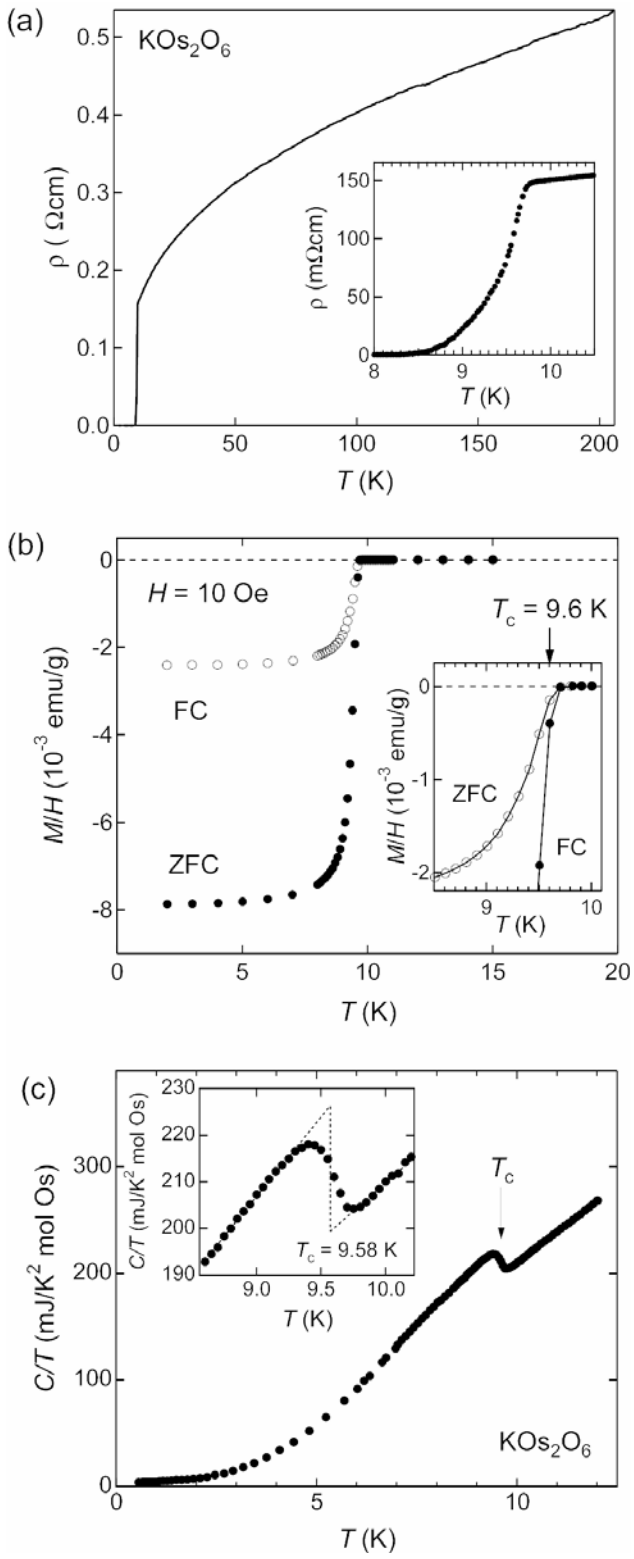


FIG. 2.

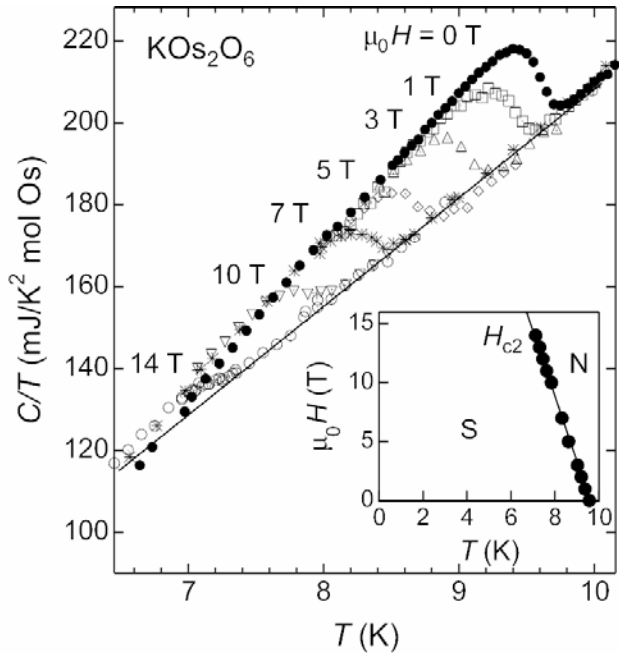


Fig. 3

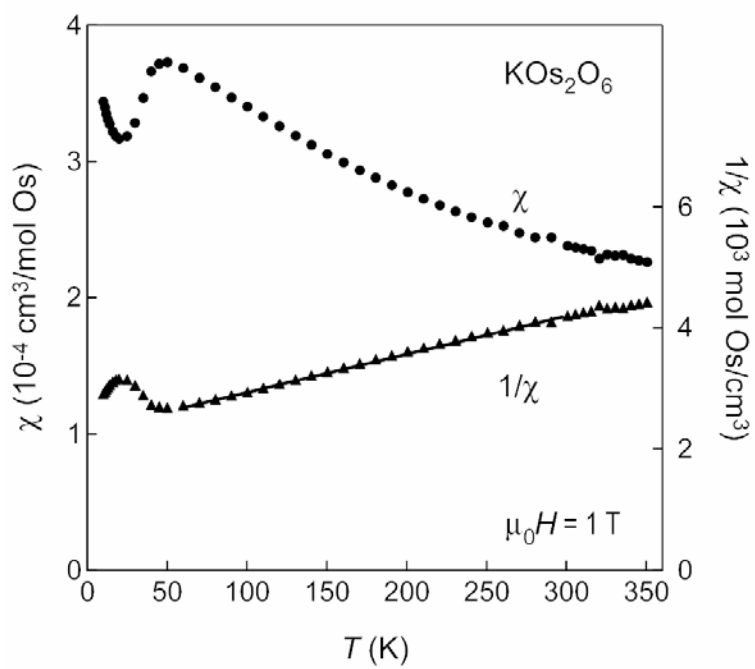


Fig. 4